



HAL
open science

reaper and bax initiate two different apoptotic pathways affecting mitochondria and antagonized by bcl-2 in *Drosophila*

Sylvain Brun, Vincent Rincheval, Sebastien Gaumer, Bernard Mignotte, Isabelle Guenal

► To cite this version:

Sylvain Brun, Vincent Rincheval, Sebastien Gaumer, Bernard Mignotte, Isabelle Guenal. reaper and bax initiate two different apoptotic pathways affecting mitochondria and antagonized by bcl-2 in *Drosophila*. *Oncogene*, 2002, 10.1038/sj.onc.1205839 . hal-03002816

HAL Id: hal-03002816

<https://hal.science/hal-03002816>

Submitted on 18 Dec 2020

HAL is a multi-disciplinary open access archive for the deposit and dissemination of scientific research documents, whether they are published or not. The documents may come from teaching and research institutions in France or abroad, or from public or private research centers.

L'archive ouverte pluridisciplinaire **HAL**, est destinée au dépôt et à la diffusion de documents scientifiques de niveau recherche, publiés ou non, émanant des établissements d'enseignement et de recherche français ou étrangers, des laboratoires publics ou privés.

reaper and *bax* initiate two different apoptotic pathways affecting mitochondria
and antagonized by *bcl-2* in *Drosophila*

Brun S., Rincheval V., Gaumer S., Mignotte B. and Guenal I.

Laboratoire de Génétique et Biologie Cellulaire, CNRS UPRES-A 8087, et Laboratoire de Génétique Moléculaire et Physiologie de l'EPHE, Université de Versailles-St Quentin en Yvelines, 45 avenue des Etats-Unis, F-78035 Versailles cedex.

Corresponding author:

Dr Isabelle GUENAL

Laboratoire de Génétique et Biologie Cellulaire,
UPRES-A 8087,
Université de Versailles-St Quentin en Yvelines,
45 avenue des Etats-Unis,
F-78035 Versailles cedex

Tel: (33) 1 39 25 36 52

Fax: (33) 1 39 25 36 55

e-mail: guenal@genetique.uvsq.fr

Running title:

bcl-2 inhibition of *reaper*-induced apoptosis

Key words:

Apoptosis, *Drosophila*, *bcl-2*, *reaper*, *bax*, mitochondria

Abstract:

bcl-2 was the first regulator of apoptosis shown to be involved in oncogenesis. Subsequent studies in mammals, in the nematode and in *Drosophila* revealed wide evolutionary conservation of the regulation of apoptosis. Although *dbok/debcl*, a member of the *bcl-2* gene family described in *Drosophila*, shows pro-apoptotic activities, no anti-apoptotic *bcl-2* family gene has been studied in *Drosophila*. We have previously reported that the human anti-apoptotic gene *bcl-2* is functional in *Drosophila*, suggesting that the fruit fly shares regulatory mechanisms with vertebrates and the nematode, involving anti-apoptotic members of the *bcl-2* family. We now report that *bcl-2* suppresses *rpr*-induced apoptosis in *Drosophila*. Additionally, we have compared features of *bax*- and *rpr*-induced apoptosis. Flow cytometry analysis of wing disc cells demonstrate that both killers trigger mitochondrial defects. Interestingly, *bcl-2* suppresses both *bax*- and *rpr*-induced mitochondrial defects while the caspase-inhibitor *p35* is specific to the *rpr* pathway. Finally, we show that the inhibition of apoptosis by *bcl-2* is associated with the down-regulation of *rpr* expression.

Introduction:

Programmed cell death by apoptosis is essential to metazoan development, metamorphosis and tissue homeostasis (Vaux & Korsmeyer, 1999). Apoptosis is a powerful biological process that removes potentially dangerous cells like self-reactive lymphocytes, virus-infected cells and tumor cells. Genetic and biochemical studies, in mammals as well as in invertebrates, reveal a high evolutionary conservation of the regulation of apoptosis. The principal executioners of apoptosis belong to a highly conserved family of proteases, the cysteinyl-aspartases (caspases). Caspases are constitutively present in cells as zymogenes, and their activation by proteolysis or auto-proteolysis provokes the cleavage of other caspases in a proteolytic activation cascade that ultimately cleaves and inactivates specific targets essential for cell structure and DNA integrity (Nunez *et al.*, 1998; Thornberry & Lazebnik, 1998). Genetic studies in *Caenorhabditis elegans* identified the genes *ced-3*, *ced-4*, *egl-1*, which are essential to trigger cell death, and *ced-9* which inhibits cell death. In cells triggered to die, the protein EGL-1 inhibits CED-9, which provokes the activation of the caspase CED-3 by CED-4 (Conradt & Horvitz, 1998). Although this model has been a scaffold for understanding the regulation of caspase activation in other species, the regulation of apoptosis in the fruit fly and in mammals shows an increased complexity compared to that in the nematode.

First, while only one caspase (CED-3) is involved in apoptosis in the nematode, at least ten caspases in mammals and seven in *Drosophila melanogaster* are involved in apoptosis (Chen *et al.*, 1998; Dorstyn *et al.*, 1999a; Dorstyn *et al.*, 1999b; Doumanis *et al.*, 2001; Fraser & Evan, 1997; Harvey *et al.*, 2001; Song *et al.*, 1997).

Second, in *C. elegans*, the regulation of apoptosis by the *bcl-2* family is mediated by the anti-apoptotic gene *ced-9* and the pro-apoptotic BH3-only gene *egl-1*. In *Drosophila* as in mammals, pro-apoptotic members of the *bcl-2* family are not limited to BH3-only genes (Gross *et al.*, 1999). Indeed, both *bcl-2* family genes identified in the fly genome are homologous to the mammalian pro-apoptotic gene *bok*, and present different BH interaction domains (Brachmann *et al.*, 2000; Colussi *et al.*, 2000; Igaki *et al.*, 2000; Zhang *et al.*, 2000). However, while *debcl/drob-1/dborg-1/dbok* has been shown to be pro-apoptotic, whether the second predicted gene of the family will be pro- or anti-apoptotic remains to be addressed.

Third, in contrast with CED-4 which constitutively activates the caspase CED-3, Apaf-1 in mammals as well as DAPAF-1/DARK/HAC-1 in the fruit fly both need ATP and cytochrome c (cyt c) as co-factors to activate caspases (Kanuka *et al.*, 1999; Li *et al.*, 1997; Rodriguez *et al.*, 1999; Zhou *et al.*, 1999). In mammals, Bax triggers the release of cyt c and

other key pro-apoptotic factors from the inter-membrane space of mitochondria like the Apoptosis Inducing Factor (AIF) and several caspases (Zamzami *et al.*, 1998), while Bcl-2 inhibits this release and apoptosis induced by Bax or many other death stimuli (Gross *et al.*, 1999). In *Drosophila*, cyt c may regulate apoptosis without being released (Dorstyn *et al.*, 2002; Varkey *et al.*, 1999; Zimmermann *et al.*, 2002). Indeed, DAPAF-1 and cyt c seem to cooperate with DRONC and DRICE in an apoptosome-like complex localized to mitochondria and responsible for the processing of both caspases DRONC and DRICE in *Drosophila* cells (Dorstyn *et al.*, 2002; Kanuka *et al.*, 1999; Li *et al.*, 1997; Rodriguez *et al.*, 1999; Zhou *et al.*, 1999). Interestingly, dBOK/DEBCL, which localizes to mitochondria, triggers cyt c release and apoptosis when expressed in mammalian cells, while in *Drosophila* cells, it triggers the translocation of DRONC to mitochondria and caspase activation without cyt c release.

In *Drosophila*, mitochondria might be targets of the three RHG domain protein RPR, HID and GRIM. Although the three genes *reaper* (*rpr*), *head involution defective* (*hid*) and *grim* are unknown in mammals, they are functional in vertebrates, and HID and GRIM localize to mitochondria during apoptosis in mammalian cells (Claveria *et al.*, 1998; Evans *et al.*, 1997; Haining *et al.*, 1999). Furthermore, in *Xenopus* cells extracts, *rpr* induces cyt c release from mitochondria (Thress *et al.*, 1999), and *bcl-2* inhibits *rpr*-dependent caspase-activation (Evans *et al.*, 1997). Zimmermann *et al.* show that *rpr*-dependent apoptosis can be independent of *dapaf-1* and cyt c *in vitro* (Zimmermann *et al.*, 2002). However, although *rpr*-dependent cyt c release is not detected in *Drosophila* cells, *dapaf-1* mutants partially suppress *rpr*-induced apoptosis, suggesting a requirement for active DAPAF-1 in the *rpr* apoptotic pathway *in vivo*.

Whether an anti-apoptotic *bcl-2* family member acts on mitochondria and cyt c to protect cells from apoptosis in *Drosophila* remains to be addressed. To our knowledge, no anti-apoptotic member of the *bcl-2* gene family has been found in the fruit fly. Nevertheless, we have shown in our laboratory that the murine pro-apoptotic gene *bax* and the human anti-apoptotic gene *bcl-2* are functional in *Drosophila melanogaster* (Gaumer *et al.*, 2000). Our current study demonstrates that *bax* and *rpr* induce two different apoptotic pathways, both affecting mitochondria. We show here that *bcl-2* suppresses *rpr*- and *bax*-induced cell death as well as *rpr*- and *bax*-induced mitochondrial defects, while the protective effect of the caspase-inhibitor *p35* is specific to the *rpr* death pathway.

Although in mammals most of the components of the cell death program are constitutively present, many apoptosis regulators in *Drosophila* are controlled at the

transcriptional level. Among others, *rpr* is transcriptionally induced to trigger apoptosis during embryonic development, metamorphosis and after X-ray irradiation (Baehrecke, 2000; Nordstrom *et al.*, 1996). In particular, after X-ray irradiation *rpr* expression is up-regulated by *dmp53*, the homologue of the mammalian oncosuppressor *p53*. Additionally, the *imd/rip* pathway, which is involved in the immune response to bacterial infection (Lemaitre *et al.*, 1995), can also trigger *rpr* expression (Georgel *et al.*, 2001). Strikingly, we also show in this paper that inhibition of apoptosis by expression of *bcl-2* during embryonic development (Gaumer *et al.*, 2000) is correlated with the down-regulation of *rpr* expression, suggesting the existence of an amplification loop in *rpr*-induced apoptosis.

Results:

A semi-quantitative approach to detect the genetic suppression of wing phenotypes.

We have used the *vg-GAL4* transgenic *Drosophila* strain to drive the expression of *UAS-rpr*, *UAS-bax* and several other transgenes in the wing margin during larval development. Flies expressing *rpr* or *bax* in the wing show two principal phenotypes: notches and wing fusion defects. We have focused on the notch phenotype to screen the flies. Surprisingly, expressivity and penetrance of the notch phenotype are variable in a population of flies of the same genotype. At 25°C, flies expressing *rpr* in the wing exhibit a distribution of phenotypes that can be classified into four categories according to their strength: strong, intermediate, weak and wildtype (figure 1). At 18°C, flies expressing *bax* in the wing exhibit a distribution of phenotypes that can be classified into three categories: strong, intermediate and weak (figure 2). Therefore, we have set a semi-quantitative approach to study genetic suppression between flies co-expressing *rpr* or *bax* and several other transgenes. To compare distributions of phenotypes between two different lineages, we have used the statistical Wilcoxon test (Wilcoxon, 1945). This test defines a *Ws* value between two populations and allows assessment of whether their distributions, which correspond to gradual phenotypes, are significantly different or not, and which population is composed of stronger phenotypes. We define the statistically significant limit as $\alpha < 10^{-3}$.

***bcl-2* and *p35* suppress *rpr*-induced cell death in the wing.**

The *Drosophila* pro-apoptotic gene *rpr* plays a key role in apoptosis. Since *bcl-2* and *rpr* have antagonistic effects on apoptosis, we tested whether the human *bcl-2* gene could suppress phenotypes induced by expression of *rpr* in the wing. Our results show that the

phenotypes induced by *rpr* are weaker when *bcl-2* is co-expressed. Although the suppression effect of *bcl-2* is partial, distributions of phenotypes clearly shift to weaker phenotypes as the number of *UAS-bcl-2* copies increases (figure 3A and table 1). Indeed, W_s values between control flies expressing only *rpr* and flies co-expressing *rpr* and one to three copies of *bcl-2* decrease from -4.1 to -9.6 ($\alpha < 10^{-3}$) as shown in table 1. Furthermore, almost 60% of flies co-expressing *rpr* and three copies of *bcl-2* show a wildtype phenotype compared to 4% of control flies. We did not find a statistical difference between distributions of phenotypes observed in flies co-expressing *rpr* and one or two copies of *bcl-2*. However, there is a significant difference between distributions of flies co-expressing *rpr* and one or two copies of *bcl-2* and the phenotype distribution of flies co-expressing *rpr* and three copies of *bcl-2* ($W_{s_{3-4}} = -6.89$; $\alpha_{3-4} = 4.6 \times 10^{-11}$). These results clearly show that *bcl-2* suppresses the phenotypes induced by *rpr* in the wing in a dose-dependent manner.

Since it has been shown that *rpr*-induced apoptosis is caspase-dependent in the developing eye (Hay *et al.*, 1995), we asked whether the caspase-inhibitor *p35* could inhibit *rpr*-induced apoptosis in the wing. Our results show that expression of *p35* partially suppresses the notches induced by *rpr* expression (figure 3B). Phenotypes of flies co-expressing *rpr* and *p35* are weaker than phenotypes of control flies, and almost 70% of flies co-expressing *rpr* and one copy of *p35* display weak or wildtype phenotypes compared to 37% of control flies. The $W_{s_{1-5}}$ value between the distributions is -5.36 and $\alpha_{1-5} < 10^{-3}$ (table 1). A second independent *p35* strain was also used to suppress *rpr*-induced cell death and both *p35* strains display similar protective activity (data not shown).

Since *bcl-2* can prevent caspase-independent cell death (Okuno *et al.*, 1998) in mammals, we have studied the co-expression of *bcl-2* and *p35* in *Drosophila*. The data presented in figure 3B and table 1 show no statistical difference between phenotype distributions of flies co-expressing *rpr* and one copy of *bcl-2*, flies co-expressing *rpr* and one copy of *p35* and flies co-expressing *rpr* and one copy of *p35* plus one copy of *bcl-2*. Consistent with this observation, we also observe no differences between the effects of two copies of *bcl-2*, one copy of *p35*, two copies of *bcl-2* plus one copy of *p35* on *rpr*-induced phenotypes (figure 3C table 1). Strikingly, while the jump from two to three copies of *UAS-bcl-2* has a great suppressive effect on the phenotypes induced by *rpr*, adding a *UAS-p35* transgene in the same genetic background has no effect. Taken together, these data show that the co-expression of both inhibitors of apoptosis has no additive effect on the phenotypes induced by *rpr*, suggesting that their inhibitory effects are somehow redundant.

***bcl-2* down-regulates *rpr* expression during embryonic development.**

Since many death signals transcriptionally induce *rpr* in cells committed to die, we asked whether *bcl-2* could only inhibit events downstream of *rpr*, or whether *bcl-2* also prevents the transcriptional induction of *rpr*. In order to determine if *bcl-2* can act upstream of *rpr*, we have used the *rpr-11-LacZ* construct (Nordstrom *et al.*, 1996) to visualize *rpr* expression during embryonic development in embryos expressing *bcl-2*. We have analyzed the X-gal staining pattern *in situ* in embryos until stage 14 of embryonic development (figure 4).

In control embryos (*rpr-11-LacZ/da-GAL4*), *LacZ* staining patterns are in agreement with those described by Nordstrom *et al.*. Interestingly, in embryos co-expressing *bcl-2* and the *LacZ* reporter (*UAS-bcl-2/+;rpr-11-LacZ/da-GAL4*), *rpr-11-LacZ* expression does not begin until stage 9 (figure 4C) while it is already detected at stage 8 in control embryos (figure 4B). At stage 9, *LacZ* staining in embryos expressing *bcl-2* is weak and only detectable in the posterior end of the extending germ band. In contrast, control embryos at a similar stage display staining at the posterior end of the extending germ band, dorsally in the region adjacent to the cephalic furrow, and more anteriorly at the clypeolabrum as well as gnathal buds (figure 4D). Subsequently, light staining is detected in segmental stripes in control embryos at stage 9 while this segmental staining does not appear until stage 10/11 in embryos expressing *bcl-2* (figure 4E). Finally, for both types of embryos, *LacZ* staining in these zones persists and intensifies from stage 11 to stage 14 (figure 4E, 4F, 4G and 4H), but *rpr* expression remains weaker in embryos expressing *bcl-2*.

In order to quantify variations of *LacZ* staining observed *in situ*, we have measured enzymatic activity of β -galactosidase in embryonic extracts at different times of development for control embryos (*rpr-11-LacZ/da-GAL4*), embryos expressing *bcl-2* (*UAS-bcl-2/+;rpr-11-LacZ/da-GAL4*) and embryos expressing *p35* (*UAS-p35/+;rpr-11-LacZ/da-GAL4*) (table 2). Activity assays were performed nine times independently, and then analyzed with the statistical Student test. For embryos of the three genotypes analyzed, our data clearly show that β -galactosidase activities are very low and not statistically different before 3h A.E.L (table 2) ($\alpha > 0.05$). Subsequently, β -galactosidase activities slightly increase 3-6h A.E.L., and become much stronger at later stages (6-9h). Indeed, for each genotype analyzed, activities measured are statistically different between the three developing times (data not shown). Strikingly, as previously observed *in situ*,

β -galactosidase activity detected is statistically lower in embryos expressing *bcl-2* than in control embryos at 3-6h and at 6-9h A.E.L. Furthermore, the activity in 3-6h-embryos expressing *bcl-2* is statistically comparable to the activity in 0-3h-control embryos (data not shown). Therefore, the 3-6h-embryos expressing *bcl-2* (including embryos at stage 8 and 9 of development) exhibit a delay in *rpr* induction, and at later stages, *rpr* expression is down-regulated in embryos expressing *bcl-2*. In contrast, expression of *p35* has no effect on *rpr* expression during embryonic development. At all developmental stages analyzed, β -galactosidase activity in embryos expressing *p35* is statistically comparable to that in control embryos (table 2). Taken together, these data argue that *bcl-2* affects the transcriptional induction of *rpr* during development, and this activity is specific to *bcl-2* since the expression of *p35* has no effect on the *rpr-11-LacZ* transgene.

***bax*-induced cell death is sensitive to *bcl-2* level but insensitive to *p35*.**

Since *p35* inhibits many *Drosophila* cell death pathways, we have tested whether *p35* could also suppress *bax*-induced phenotypes. As previously described, *bax*-induced phenotypes are variable at 18°C. The severity of wing notches ranges from strong to weak phenotypes (figure 2). To study genetic interactions between *bax* and *bcl-2* or *p35*, females carrying both the *vg-GAL4* driver and *UAS-bax* (*vg-GAL4,UAS-bax/CyO-gfp*) were crossed to males carrying copies of the *UAS-bcl-2* or *UAS-p35* transgenes. Results are presented in figure 5, and distributions of phenotypes are compared using the statistical Wilcoxon test (table 3 and 4).

Distributions of phenotypes between females co-expressing *bax* and *p35* and females expressing *bax* but not *p35* are not statistically different ($W_{S_{1-2}}=-0.79$; $\alpha_{1-2}=0.43$). This result is comparable to that in male lineages: $W_{S_{5-6}}=2.55$; $\alpha_{5-6}=0.01$. A similar result was obtained using a different *UAS-p35* transgenic strain as well as a third strain carrying two copies of *UAS-p35* (data not shown). Note that the different *p35* strains suppress *rpr*-induced cell death in the wing (figure 3 and data not shown). In contrast, *bax* is sensitive to *bcl-2* level and the strength of *bax*-induced phenotypes decreases as the number of *bcl-2* copies increases. Indeed, 73% of females and 41% of males co-expressing *bax* and one copy of *bcl-2* have weak phenotypes compared respectively to 10% of females and 15% of males expressing only *bax*. Moreover, females co-expressing *bax* and three copies of *bcl-2* have weaker phenotypes than those co-expressing a single copy of *bcl-2* ($W_{S_{3-4}}=-3.76$; $\alpha_{3-4}<10^{-3}$). Similarly, two copies of *bcl-2* in male lineage suppress phenotypes induced by *bax* more effectively than one copy

($W_{S7-8} = -5.97$; $\alpha_{7-8} < 10^{-3}$). In these experiments, *bcl-2* suppresses phenotypes induced by *bax* in a dose-dependent manner while *p35* has no effect. These data suggest that *bcl-2* inhibits apoptosis triggered through a *p35*-insensitive pathway in the fly.

Wing discs are differently affected by *bax* and *rpr* expression

As shown in figure 6, acridine orange (AO) staining of wing discs of third instar larvae expressing *rpr* or *bax* driven by *vg-GAL4* shows prominent apoptosis, while in wildtype discs, apoptosis is very low and appears preferentially in the notum (figure 6). Staining in discs expressing *rpr* is intense and foreshadows *vg-GAL4* expression. More central labeling is detectable in discs expressing *bax*, though most of AO staining is also found in the area of *vg-GAL4* expression. This discrepancy of staining pattern suggests that although massive apoptosis occurs in discs expressing *rpr* like in discs expressing *bax*, the wing pouch of the disc is more affected by *bax* expression. Additionally, expression of *bax* or *rpr* triggers a dramatic decrease of disc size. Thus, both reduced size of discs and AO staining pattern show that *rpr*- and *bax*-induced apoptosis occur at least before as well as within the third instar larval stage of development.

***bax* and *rpr* induce mitochondrial membrane potential collapse, cell shrinkage but no necrosis**

It has been shown in mammalian cells and recently in *Drosophila* cells that mitochondrial membrane potential ($\Delta\Psi_m$) drop is an early event in apoptosis when compared to DNA fragmentation and plasma membrane injuries (Vayssière *et al.*, 1994; Zimmermann *et al.*, 2002). Therefore, we asked whether *rpr*- and *bax*-induced cell death *in vivo* in *Drosophila* provoke $\Delta\Psi_m$ collapse. Flow cytometry analyses were carried out to study the integrity of the plasma membrane, variations of $\Delta\Psi_m$ and cell shrinkage in third instar larvae wing discs. We have used Propidium Iodide (PI) which penetrates only cells with a loss of membrane integrity, like necrotic cells or late apoptotic cells, as a specific indicator of cell membrane integrity. We have assessed mitochondrial membrane potential using DiOC₆(3), a lipophilic cation taken up by mitochondria in proportion to $\Delta\Psi_m$, and cell shrinkage was analyzed by observing cell size reduction. Results presented for the study of *bax*-induced apoptosis and for the study of *rpr*-induced apoptosis are taken from independent experiments. In both studies, assays on cells isolated from discs carrying the death inducer without a driver (control discs) or from discs expressing the death inducer alone or co-expressing the death inducer and *p35*

or *bcl-2* have been performed in parallel. Only cytograms corresponding to cells of genotype (*UAS-rpr/X*) and (*UAS-rpr/X;vg-GAL4/+*) are presented (figure 7A). For each sample analyzed, cell debris and aggregates as well as PI-positive cells are excluded from the DiOC₆(3) analysis.

In *rpr* control discs (figure 7Aa), 6% of cells show high PI fluorescence (window P) and PI-negative cells with no major membrane injuries split into two distinct populations based on their DiOC₆(3) fluorescence and their size (figure 7Ab): 84% of cells have a large size and high DiOC₆(3) fluorescence (figure 7Ab, window H), while other dots in window L characterize cells with a reduced size and $\Delta\Psi_m$ drop. These 16% of cells in window L exhibit characteristics of apoptosis: they undergo $\Delta\Psi_m$ collapse and cell shrinkage while their plasma membrane is not permeable. Moreover, as demonstrated below, expression of each death inducer *rpr* or *bax* increases this apoptotic population. Thus, we observe a background level of apoptotic cells in control discs, which is in agreement with *in situ* observation of normal developmental apoptosis by AO staining of wildtype wing discs (figure 6B). In addition, the dissociation process, performed to obtain individual disc cells, probably deprives cells of survival signals, thus accelerating commitment to apoptosis (see materials and methods). Therefore, since experimental procedures as well as markers used for *in situ* labeling and *in vitro* measurements are different, the results from both types of experiments are not quantitatively comparable.

However, it is clear that discs expressing *rpr* or *bax* exhibit a significant increase in the portion of apoptotic cells. Thus, in order to estimate apoptosis triggered by expression of *rpr* or *bax*, we have subtracted the background level of apoptosis occurring in control discs (window L) from apoptosis measured in discs expressing *rpr* or *bax* (figure 7C). This analysis shows that expression of *rpr* induces $\Delta\Psi_m$ drop and cell shrinkage. Indeed, only 63% of cells in discs expressing *rpr* maintain high DiOC₆(3) fluorescence (window H), versus 84% in control discs (figure 7Ab and d). In discs expressing *rpr*, 21% more cells undergo apoptosis than in control discs (figure 7C), while almost none become PI-positive (figure 7Ac). Consistent with the *in situ* observations, equivalent results are obtained when *bax* is expressed (figure 7B and C). We observe 8% of PI positive cells in *bax* expressing discs and 7% in *bax* control discs, showing that *bax* expression does not induce necrosis. Moreover, *bax* induces 22% more apoptosis than in control discs (figure 7C). This quite low apoptogenic effect of *rpr* and *bax* is likely due to the restricted *vg-GAL4* expression in the wing disc (figure 6A).

Indeed, flow cytometry analysis of (*vg-GAL4/UAS-gfp*) third instar larvae shows that only 30% of cells in wing discs are positive for Green Fluorescent Protein (data not shown).

bcl-2* suppresses $\Delta\Psi_m$ collapse induced by *bax* and *rpr*, while *p35* activity is specific to *rpr

In order to characterize the effect of *bcl-2* and *p35* on $\Delta\Psi_m$ collapse specifically triggered by *bax* and *rpr*, we have studied the co-expression of *bax* or *rpr* with *p35* or *bcl-2* (figure 7B and C). Control discs and discs co-expressing *rpr* and *bcl-2* display similar numbers of apoptotic cells (e.i. cells with a low $\Delta\Psi_m$ and a decrease in size) (16% and 15% respectively) (figure 7B). When *rpr* and *p35* are co-expressed, only 13% more cells than in controls undergo apoptosis (figure 7C) compared to 21% more when only *rpr* is expressed. These data argue that *p35* protects more than half of the cells triggered to die by *rpr*, and *bcl-2* completely restores wildtype mitochondrial phenotype.

In wing discs over-expressing *bax*, 22% more cells undergo apoptosis than in *bax* control discs. When *bcl-2* and *bax* are co-expressed, only 6% more cells undergo apoptosis than in controls (figure 7C). In contrast, the percentage of cells undergoing apoptosis in discs co-expressing *bax* and *p35* remains similar to discs expressing *bax* but not *p35* (38% and 40% respectively) (figure 7B). Therefore, *p35* has no effect on *bax*-induced cell shrinkage and $\Delta\Psi_m$ drop. Taken together these results demonstrate that both *bcl-2* and *p35* can protect cells from $\Delta\Psi_m$ drop and cell shrinkage, but while *bcl-2* is effective against both *bax*- and *rpr*-induced defects, *p35* protection is specific to *rpr*-induced effect.

Discussion:

To further characterize the genetic regulation of apoptosis, we have used the *UAS/GAL4* system to express mammalian regulators of apoptosis in *Drosophila*. Specifically, we have studied the genetic interactions between the human anti-apoptotic gene *bcl-2* with the *Drosophila* death pathway controlled by *rpr*. In addition, we have compared apoptosis induced by the *Drosophila* gene *rpr* and the murine gene *bax* in the wing margin during development. Since both killers induce a notch phenotype with variable expressivity, we have set a semi-quantitative approach to compare distributions of gradual phenotypes between different genotypes. As the classification of the phenotypes might depend on the observer, the suppression analysis has only been performed on progeny from crosses performed in parallel

and carefully analyzed by a single blind observer. Therefore, we have not compared distributions from independent sets of experiments. However, we have analyzed the distributions of wing phenotypes of flies expressing *bax* in six independent experiments, and 5/6 distributions compared using the Wilcoxon test were statistically similar. Only one distribution analyzed was statistically different from four others (data not shown). Additionally, the effects observed in our experiments are not likely to be mediated by the titration of the GAL4 activator by *UAS* elements. Indeed, we show that there is no additive effect on the phenotypes induced by *UAS-rpr* when the *UAS-p35* transgene is added to one or two *UAS-bcl-2* transgenes. Furthermore, two independent *UAS-p35* insertions, alone or together, have no effect on the phenotypes induced by *UAS-bax* (data not shown). This method has proven to be very powerful in detecting gradual suppression effects that a classical dichotomy screen can not detect.

In this study, we have focused on the involvement of mitochondria as well as the *bcl-2* gene family in apoptosis in *Drosophila melanogaster*. In mammals, *bax* triggers apoptosis by permeabilizing the outer mitochondrial membrane. This permeabilization is correlated with mitochondrial membrane potential ($\Delta\Psi_m$) drop and cyt c release (Desagher & Martinou, 2000). *rpr* is also thought to act on mitochondria. Indeed, in *Xenopus* cells extracts, RPR binds to Scythe to induce cyt c release from purified mitochondria (Thress *et al.*, 1999). We report here that expression of *bax* or *rpr* in the wing margin during development induces apoptosis, and flow cytometry experiments performed on dissociated wing disc cells show that *bax* and *rpr* trigger $\Delta\Psi_m$ drop and cell shrinkage *in vivo* in *Drosophila*. These results point to mitochondrial changes as common events in *bax* and *rpr* death pathways in *Drosophila* (figure 8). Moreover, *bax* and *rpr* do not induce necrosis and late apoptotic cells or bodies are likely phagocytosed *in vivo* as previously reported (Milan *et al.*, 1997). Nevertheless, several features differentiate *bax*- and *rpr*-induced apoptosis. Although *bax* and *rpr* induce comparable decrease in wing disc size, massive AO staining, as well as comparable apoptogenic effect (about 20%), adult phenotypes are much stronger after *bax* expression. One explanation could be that *bax*-induced apoptosis is irreversible while some of the cells initially triggered by *rpr* and showing $\Delta\Psi_m$ collapse ultimately do not undergo apoptosis. Since AO staining is prominent in *rpr* as well as *bax* expressing discs, and given that AO likely stains cells which are committed to apoptosis, this hypothesis appears unlikely. In addition, as shown by AO staining *in situ*, the wing pouch of third instar larvae is more affected by *bax* expression than by *rpr* expression. This result suggests that earlier during

development, cells in the wing disc respond differently to both death inducers. Since cells of the wing pouch give rise to the adult wing blade (Bate & Martinez Arias, 1993), it is likely that adult flies expressing *bax* present stronger wing phenotypes. Finally, when cell death is induced in the wing during larval and pupal development, the adult phenotype is also dependent on compensation mechanisms triggered in order to recover normal wing (Milan *et al.*, 1997). Therefore, we can not exclude that this process respond differently to *bax*- and *rpr*-induced apoptosis.

It has already been shown that *rpr*-induced apoptosis in the eye is caspase-dependent (Hay *et al.*, 1995). To test the requirement of caspases in *bax* and *rpr* apoptotic pathways in the wing, we have studied their genetic interactions with the caspase-inhibitor *p35*. We show here that cell death triggered by *rpr* in the wing involves cell shrinkage and mitochondrial defects, and that this process is caspase-dependent. In contrast, *p35* has no effect on mitochondrial changes triggered by *bax*. Moreover, we have never observed any inhibitory effect of *p35* on *bax*-induced apoptosis in the wing by using two independent *p35*-transgenic lines, and a third line carrying two copies of *p35*. The inability of *p35* to suppress the *bax* death pathway may be due to the activation of *p35*-insensitive caspases or to the activation of caspase-independent events. In mammals, it remains controversial whether *bax*-induced cell death is caspase-dependent (Okuno *et al.*, 1998; Vekrellis *et al.*, 1997; Xiang *et al.*, 1996). In *Drosophila*, it is also not clear whether the pro-apoptotic *bcl-2* family gene *dbok/debcl* acts in a caspase-dependent death pathway (Chen & Abrams, 2000; Zimmermann *et al.*, 2002). In our experiments, *bcl-2* inhibits *bax*- as well as *rpr*-induced phenotypes in a dose-dependent manner, and *bcl-2* inhibits $\Delta\Psi_m$ drop and cell shrinkage induced by *bax* and *rpr* *in vivo*. Taken together, our data suggest that *bax* and *rpr* induce two different death pathways, though mitochondrial defects as well as the inhibition by *bcl-2* constitute two common features of *rpr*- and *bax*-induced apoptosis (figure 8).

Taking into account what occurs *in vitro*, we hypothesize that *bcl-2* can inhibit *rpr*- and *bax*-induced apoptosis by regulating cyt c-dependent DAPAF-1 activation. But in this case, since we have shown that *p35* does not counteract *bax*, the caspases regulated by DAPAF-1 would be *p35*-insensitive. DREDD cleavage (possibly by auto-activation), DRONC activity in the eye as well as STRICA-induced cell death are not inhibited by *p35* (Chen *et al.*, 1998; Doumanis *et al.*, 2001; Hawkins *et al.*, 2000). Therefore, these caspases are good candidates for potential members of a *bax*-induced cell death pathway. In addition, consistent with what occurs in mammals (Okuno *et al.*, 1998), we show that in *Drosophila*,

bcl-2 suppresses caspase-dependent and -independent apoptotic mitochondrial events and apoptosis.

Our results are the first evidence of a protective activity of *bcl-2* against *rpr*-induced apoptosis *in vivo* in *Drosophila*. Since *bcl-2* can prevent caspase-independent cell death in mammals (Okuno *et al.*, 1998), we have studied the effect of the co-expression of *bcl-2* and *p35* on *rpr*-induced adult wing phenotypes. We show that there is no additive effect of *p35* and *bcl-2* when they are co-expressed. This data suggests that *bcl-2* and *p35* do not inhibit completely different pathways, and that *bcl-2* could affect the activation of *p35*-sensitive caspases downstream of *rpr* expression. Furthermore, we show that *p35* suppresses $\Delta\Psi_m$ collapse induced by *rpr*, which suggests that *p35*-sensitive caspases act on mitochondria (figure 8). This data is in agreement with Varkey *et al.* who have shown that *rpr*-induced cyt c modifications are caspase-dependent (Varkey *et al.*, 1999). Nevertheless, we do not know whether the action of these *p35*-sensitive caspases initiates a mitochondrial apoptotic pathway, or whether it is the result of positive feedback involving these caspases, which would accelerate mitochondrial dysfunction.

Finally, while *bcl-2* displays anti-apoptotic properties related to an activity downstream of *rpr*, we also show here that *bcl-2* can act by regulating *rpr* transcriptional induction. This is the first evidence of the action of the *bcl-2* gene family on the expression of *rpr*. In regards to the current knowledge of the genetic regulation of apoptosis, and considering our results, it is likely that the human gene *bcl-2* acts on mitochondria in *Drosophila* to inhibit apoptosis triggered by *rpr* or by *bax* (figure 8). However, exactly how *bcl-2* down-regulates *rpr* expression remains to be addressed. One can ask whether this effect is cell-autonomous. Indeed, in embryos, cells committed to die may sensitize neighbor cells and increase their level of *rpr* product. By decreasing the number of apoptotic cells, *bcl-2* would reduce *rpr* expression. Nevertheless, since *p35* has no effect on *rpr* expression during embryonic development, it is unlikely that the effect of *bcl-2* is due to such a non cell-autonomous activity.

Until recently, two death signals were known to be involved in the regulation of *rpr* expression. First, *rpr* is a transcriptional target of the steroid hormone ecdysone during metamorphosis (Baehrecke, 2000), but to our knowledge, no interaction between *bcl-2* and steroid-induced gene expression has been described. Second, it has been shown that *rpr* is a transcriptional target of *dmp53* after X-ray irradiation (Brodsky *et al.*, 2000). Similarly, in mammals, the transcription factor NF-kappaB is involved in cell proliferation as well as in oncogenesis (Rayet & Gelinas, 1999), and among the many target genes of NF-kappaB are

p53 and *c-myc*. In *Drosophila*, a death domain protein that promotes apoptosis, *imd/rip*, and a homologue of a mammalian member of the death domain receptor pathway, *dfadd*, have been recently characterized (Georgel *et al.*, 2001; Hu & Yang, 2000). Both of them interact with *dredd/caspase-8*, which suggests that a death domain receptor pathway that utilizes caspase-mediated NF-kappaB activation of *rpr* transcription could regulate apoptosis (figure 7). Our results suggest that this feedback control of *rpr* expression should be sensitive to *bcl-2* but not to *p35*. Whether *bcl-2* activates or inhibits NF-kappaB to regulate apoptosis remains controversial (De Moissac *et al.*, 1998; Grimm *et al.*, 1996; Hour *et al.*, 2000). Since *rpr* expression is affected by *imd/rip*, *dmp53* and *bcl-2*, genetic interaction studies between these genes will be of great interest to better understand the link between the *rel/NF-κB* gene family and the regulation of apoptosis by *p53*, *bcl-2* and death domain receptors such as the TNFα-receptors in *Drosophila*, and in mammals. More generally, since no anti-apoptotic *bcl-2* has been studied in *Drosophila*, further studies of the human anti-apoptotic *bcl-2* gene in the fly will give new insights into the regulation of apoptosis by the *bcl-2* family, and delineate new strategies for the design of chemotherapeutic apoptosis inducers which are insensitive to the *bcl-2* oncogene.

Materials and methods:

Fly stocks:

Flies were raised on standard medium. Both driver strains used in this study, *vestigial-GAL4* (*vg-GAL4*) and *daughterless-GAL4* (*da-GAL4*) as well as the (UAS-*gfp*) strain (UAS: Upstream Activating Sequence) were described previously (Gaumer *et al.*, 2000). The strains carrying *UAS-p35*, *UAS-bax* and *UAS-bcl-2* transgenes have been generated in our laboratory and were described previously (Gaumer *et al.*, 2000). The *rpr-11-LacZ* construct was first described by Nordstrom *et al* (Nordstrom *et al.*, 1996). The fly stock carrying the *UAS-rpr* transgene was generated by recombination of the X-linked (*UAS-rpr*, *UAS-hid*) strain described previously (Zhou *et al.*, 1997). We used *w¹¹¹⁸* Canton S fly stock as the reference strain.

rpr suppression study:

Males (*UAS-rpr/Y*), (*UAS-rpr/Y;vg-GAL4/CyO*) or (*UAS-rpr/Y;UAS-p35*) were crossed at 25°C to females of the following strains: (*vg-GAL4*), (*vg-GAL4;UAS-bcl-2*), (*UAS-bcl-2;vg-GAL4;UAS-bcl-2*), (*UAS-bcl-2;UAS-bcl-2;UAS-bcl-2*). The progeny were then

raised at 25°C and females expressing *UAS-rpr* were analyzed within the first day after eclosion to prevent wings from being damaged.

***bax* suppression study:**

Females (*vg-GAL4,UAS-bax/CyO-gfp*) (GFP: Green fluorescent protein) were crossed at 18°C to males of the following strains: (*w¹¹¹⁸*), (*UAS-bcl-2*), (*UAS-p35*), (*UAS-bcl-2/Y;UAS-bcl-2;UAS-bcl-2*). The progeny were raised at 18°C and analyzed every day.

Classification of the phenotypes and the Wilcoxon test:

The principle of the phenotype classification was different in the *rpr* suppression study and in the *bax* suppression study. Note that in both sets of experiments, all the lineages were analyzed in parallel and by a blind observer. In the *rpr* suppression study, flies were classified in four different phenotypic categories according to their wing phenotype: strong, intermediate, weak and wildtype (figure 1). For flies showing two different wings, the strongest phenotype of both wings was used for the classification. In the *bax* suppression study, flies were classified in the «strong» category when both wings had strong phenotypes, in the «weak» category when both wings had weak phenotypes and in the «intermediate» category when it did not belong to either the «strong» or «weak» category (figure 2).

In our experiments we have analyzed the distribution of graded phenotypes based on their expressivity. The Wilcoxon test was used to compare the distributions of the phenotypes between two lineages A and B (Wilcoxon, 1945) (table 1, 3 and 4). The sign of $W_{S_{A-B}}$ value determines whether the distribution A is stronger than B ($W_s < 0$) or whether the distribution B is stronger than A ($W_s > 0$). We considered the difference between A and B significant when $\alpha_{A-B} < 10^{-3}$.

Staining of embryos with X-gal:

Females (*UAS-bcl-2;da-GAL4*) or (*da-GAL4*) were crossed to males (*rpr-11-LacZ*) at 25°C. Embryos were dechorionated 5 min in 1X bleach and rinsed in water. Embryos were fixed 10 min in 1X PBS pH 7.6, 3.7% formaldehyde/heptane (1:2) and washed four times in 1X PBS pH 7.6, 0.3% triton X-100. The embryos were stained for 15 to 25 min in 1X PBS pH 7.6, K_4Fe_2 4 mM, K_3Fe_3 4 mM, $MgCl_2$ 1 mM, 1% triton X-100, X-gal 560 $\mu\text{g}\cdot\text{ml}^{-1}$ (Eurogentec), fixed 3 min in 1X PBS pH 7.6, 3.7% formaldehyde and washed three times in 1X PBS pH 7.6, 0.05% triton X-100. The embryos were swelled over night in

1X PBS pH 7.6, 0.05% triton X-100/glycerol (40:60) and finally mounted in glycerol. Embryos were staged according to Campos-Ortega and Hartenstein (Campos-Ortega & Hartenstein, 1985). Samples were observed with a conventional research microscope DMRHC Leica.

β -galactosidase activity assay:

Females (*UAS-bcl-2;da-GAL4*), (*UAS-p35;da-GAL4*) or (*da-GAL4*) were crossed to males (*rpr-11-LacZ*) at 25°C. Embryos were collected at different development times A.E.L and harvested in 500 μ l buffer Z (described by Tzou *et al.* (Tzou *et al.*, in press)). The final concentration of proteins in extracts was $138 \pm 87 \mu\text{g.ml}^{-1}$ (n=81), and the final concentration of ONPG (Sigma) for the β -galactosidase activity assay was 0.35 mg.ml^{-1} . The kinetics of ONPG hydrolysis were measured over 6h. The activity assays for each genotype analyzed and at all development time segments were performed nine times independently (table 2). The measured activities were compared using the statistical Student test.

Detection of *vg-GAL4* expression in wing discs:

Females (*vg-GAL4*) were crossed to (*UAS-gfp*) males. (*vg-GAL4/UAS-gfp*) lineage was raised at 25°C and third instar larvae were dissected and mounted in 1X PBS pH 7.6. Discs were then observed with a conventional research microscope DMRHC Leica using the L5 filter to detect green fluorescence.

AO staining of wing discs:

Females (*UAS-rpr*) or (*UAS-bax,vg-GAL4/CyO-gfp*) were crossed respectively to (*vg-GAL4*) or (*w¹¹¹⁸*) males. (*UAS-rpr/+;vg-GAL4/+*) lineage was raised at 25°C and (*UAS-bax,vg-GAL4/+*) as well as (*w¹¹¹⁸*) lineage were raised at 21°C. Third instar larvae were dissected in 1X PBS pH 7.6 and stained for 2 minutes in (100 ng.ml⁻¹) Acridine Orange (Molecular Probes). Discs were then mounted in PBS and observed with a conventional research microscope DMRHC Leica using the I3 filter to detect green fluorescence.

Flow cytometry analysis:

Males (*UAS-rpr/Y*) or (*UAS-bax/CyO-gfp*) were crossed respectively at 25°C and 21°C to females of the following strains: (*w¹¹¹⁸*), (*vg-GAL4*), (*UAS-bcl-2;vg-GAL4;UAS-bcl-2*), (*vg-GAL4;UAS-p35*). Progeny were raised at the same temperatures. Wing discs from third instar female larvae were dissected in 1X PBS pH 7.6,

and pooled in Schneider's *Drosophila* medium (GibcoBRL). Six discs were pooled per sample. The discs were then incubated in 150 μ L Trypsine (GibcoBRL) for 1h30 at 28°C. The reaction was stopped by adding 10 μ L Fetal Calf Serum (FCS). The samples were stained at room temperature in Schneider's *Drosophila* medium for 30 min in 0.1 μ M DiOC₆(3), and for 5 min in 50 μ g.mL⁻¹ Propidium Iodide (PI) (final volume of 500 μ L). Samples were preserved on ice before analysis. The cationic lipophilic fluorochrome DiOC₆(3) (Molecular Probes) is a cell permeable marker which at low doses (0.1 μ M), specifically accumulates in mitochondria in mammalian cells in proportion to $\Delta\Psi_m$ (Petit *et al.*, 1990). PI (Sigma) is a non specific DNA intercalating agent which is excluded by the plasma membrane of living cells.

Flow cytometry measurements were performed on a XL3C flow cytometer (Beckman-Coulter France). Fluorescence excitation was obtained using the blue wavelength (488nm) of an argon ion laser operating at 15mW. Green fluorescence of DiOC₆(3) was collected with a 525nm band pass filter and red fluorescence of PI with a 620nm band pass filter. Analyses were performed on 10⁴ cells and data were stored in listmode. Light scattering values were measured on a linear scale of 1024 channels and fluorescence intensities on a logarithmic scale of fluorescence.

Acknowledgements:

We are grateful to Dr G. Lecellier for expert help with statistics. We also thank E. Blanchardon who provided us the (*UAS-rpr*) strain, Imène Seninet for technical help, Dr L. Theodore for helpful discussions and M.R. Watson for her critical reading of the manuscript. This work was supported in part by grants from the Association pour la Recherche contre le Cancer (#4480) and from the Ligue Contre le Cancer (Comité des Yvelines). S. Brun was a recipient of a fellowship from the Ministère de l'Education Nationale et de l'Enseignement Supérieur et de la Recherche. S. Gaumer was supported by a fellowship from the Association pour la Recherche contre le Cancer.

References:

- Baehrecke, E.H. (2000). *Cell Death Differ.*, **7**, 1057-1062.
- Bate, M. & Martinez Arias, A. *The development of Drosophila melanogaster*. Cold Spring Harbor Laboratory Press.
- Brachmann, C.B., Jassim, O.W., Wachsmuth, B.D. & Cagan, R.L. (2000). *Curr. Biol.*, **10**, 547-550.

- Brodsky, M.H., Nordstrom, W., Tsang, G., Kwan, E., Rubin, G.M. & Abrams, J.M. (2000). *Cell*, **101**, 103-113.
- Campos-Ortega, J.A. & Hartenstein, V. *The embryonic development of Drosophila melanogaster*. Springer-Verlag, Berlin.
- Chen, P. & Abrams, J.M. (2000). *J. Cell Biol.*, **148**, 625-627.
- Chen, P., Rodriguez, A., Erskine, R., Thach, T. & Abrams, J.M. (1998). *Dev. Biol.*, **201**, 202-216.
- Claveria, C., Albar, J.P., Serrano, A., Buesa, J.M., Barbero, J.L., Martinez, A.C. & Torres, M. (1998). *EMBO J.*, **17**, 7199-7208.
- Colussi, P.A., Quinn, L.M., Huang, D.C., Coombe, M., Read, S.H., Richardson, H. & Kumar, S. (2000). *J. Cell Biol.*, **148**, 703-714.
- Conradt, B. & Horvitz, H.R. (1998). *Cell*, **93**, 519-529.
- De Moissac, D., Mustapha, S., Greenberg, A.H. & Kirshenbaum, L.A. (1998). *J. Biol. Chem.*, **273**, 23946-23951.
- Desagher, S. & Martinou, J.C. (2000). *Trends Cell Biol.*, **10**, 369-377.
- Dorstyn, L., Colussi, P.A., Quinn, L.M., Richardson, H. & Kumar, S. (1999a). *Proc. Natl. Acad. Sci. USA*, **96**, 4307-4312.
- Dorstyn, L., Read, S., Cakouros, D., Huh, J.R., Hay, B.A. & Kumar, S. (2002). *J. Cell Biol.*, **156**, 1089-1098.
- Dorstyn, L., Read, S.H., Quinn, L.M., Richardson, H. & Kumar, S. (1999b). *J. Biol. Chem.*, **274**, 30778-30783.
- Doumanis, J., Quinn, L., Richardson, H. & Kumar, S. (2001). *Cell Death Differ.*, **8**, 387-394.
- Evans, E.K., Kuwana, T., Strum, S.L., Smith, J.J., Newmeyer, D.D. & Kornbluth, S. (1997). *EMBO J.*, **16**, 7372-7381.
- Fraser, A.G. & Evan, G.I. (1997). *EMBO J.*, **16**, 2805-2813.
- Gaumer, S., Guéna, I., Brun, S., Théodore, L. & Mignotte, B. (2000). *Cell Death Differ.*, **7**, 804-814.
- Georgel, P., Naitza, S., Kappler, C., Ferrandon, D., Zachary, D., Swimmer, C., Kopczynski, C., Duyk, G., Reichhart, J.M. & Hoffmann, J.A. (2001). *Dev. Cell*, **1**, 503-514.
- Grimm, S., Bauer, M.K., Baeuerle, P.A. & Schulze-Osthoff, K. (1996). *J. Cell Biol.*, **134**, 13-23.
- Gross, A., McDonnell, J.M. & Korsmeyer, S.J. (1999). *Genes Dev.*, **13**, 1899-1911.
- Haining, W.N., Carboy-Newcomb, C., Wei, C.L. & Steller, H. (1999). *Proc. Natl. Acad. Sci. USA*, **96**, 4936-4941.
- Harvey, N.L., Daish, T., Mills, K., Dorstyn, L., Quinn, L.M., Read, S.H., Richardson, H. & Kumar, S. (2001). *J. Biol. Chem.*, **276**, 25342-25350.
- Hawkins, C.J., Yoo, S.J., Peterson, E.P., Wang, S.L., Vernoooy, S.Y. & Hay, B.A. (2000). *J. Biol. Chem.*, **275**, 27084-27093.
- Hay, B.A., Wassarman, D.A. & Rubin, G.M. (1995). *Cell*, **83**, 1253-1262.
- Hour, T.C., Chen, L. & Lin, J.K. (2000). *Eur. J. Cell Biol.*, **79**, 121-129.
- Hu, S. & Yang, X. (2000). *J. Biol. Chem.*, **275**, 30761-30764.
- Igaki, T., Kanuka, H., Inohara, N., Sawamoto, K., Nunez, G., Okano, H. & Miura, M. (2000). *Proc. Natl. Acad. Sci. USA*, **97**, 662-667.

- Kanuka, H., Sawamoto, K., Inohara, N., Matsuno, K., Okano, H. & Miura, M. (1999). *Mol. Cell*, **4**, 757-769.
- Lemaitre, B., Kromer-Metzger, E., Michaut, L., Nicolas, E., Meister, M., Georgel, P., Reichhart, J.M. & Hoffmann, J.A. (1995). *Proc. Natl. Acad. Sci. U S A*, **92**, 9465-9469.
- Li, P., Nijhawan, D., Budihardjo, I., Srinivasula, S.M., Ahmad, M., Alnemri, E.S. & Wang, X. (1997). *Cell*, **91**, 479-489.
- Milan, M., Campuzano, S. & Garcia-Bellido, A. (1997). *Proc. Natl. Acad. Sci. USA*, **94**, 5691-5696.
- Nordstrom, W., Chen, P., Steller, H. & Abrams, J.M. (1996). *Dev. Biol.*, **180**, 213-226.
- Nunez, G., Benedict, M.A., Hu, Y. & Inohara, N. (1998). *Oncogene*, **24**, 3237-3245.
- Okuno, S., Shimizu, S., Ito, T., Nomura, M., Hamada, E., Tsujimoto, Y. & Matsuda, H. (1998). *J. Biol. Chem.*, **273**, 34272-34277.
- Petit, P.X., O'Connor, J., Grunwald, D. & Brown, S.C. (1990). *Eur. J. Biochem.*, **194**, 389-397.
- Rayet, B. & Gelinis, C. (1999). *Oncogene*, **18**, 6938-6947.
- Rodriguez, A., Oliver, H., Zou, H., Chen, P., Wang, X. & Abrams, J.M. (1999). *Nat. Cell Biol.*, **1**, 272-279.
- Song, Z., McCall, K. & Steller, H. (1997). *Science*, **275**, 536-540.
- Thornberry, N.A. & Lazebnik, Y. (1998). *Science*, **281**, 1312-1316.
- Thress, K., Evans, E.K. & Kornbluth, S. (1999). *EMBO J.*, **18**, 5486-5493.
- Tzou, P., Meister, M. & Lemaitre, B. (in press). *Methods in Microbiology*, **31**, 507-529.
- Varkey, J., Chen, P., Jemmerson, R. & Abrams, J.M. (1999). *J. Cell Biol.*, **144**, 701-710.
- Vaux, D.L. & Korsmeyer, S.J. (1999). *Cell*, **96**, 245-254.
- Vayssière, J.L., Petit, P.X., Risler, Y. & Mignotte, B. (1994). *Proc. Natl. Acad. Sci. USA*, **91**, 11752-11756.
- Vekrellis, K., McCarthy, M.J., Watson, A., Whitfield, J., Rubin, L.L. & Ham, J. (1997). *Development*, **124**, 1239-1249.
- Wilcoxon, F. (1945). *Biometrics*, **1**, 80-83.
- Xiang, J., Chao, D.T. & Korsmeyer, S.J. (1996). *Proc. Natl. Acad. Sci. USA*, **93**, 14559-14563.
- Zamzami, N., Brenner, C., Marzo, I., Susin, S.A. & Kroemer, G. (1998). *Oncogene*, **16**, 2265-2282.
- Zhang, H., Huang, Q., Ke, N., Matsuyama, S., Hammock, B., Godzik, A. & Reed, J.C. (2000). *J. Biol. Chem.*, **275**, 27303-27306.
- Zhou, L., Schnitzler, A., Agapite, J., Schwartz, L.M., Steller, H. & Nambu, J.R. (1997). *Proc. Natl. Acad. Sci. USA*, **94**, 5131-5136.
- Zhou, L., Song, Z., Tittel, J. & Steller, H. (1999). *Mol. Cell*, **4**, 745-755.
- Zimmermann, K.C., Ricci, J.E., Droin, N.M. & Green, D.R. (2002). *J. Cell Biol.*, **156**, 1077-1087.

Table 1: Ws values and α values of the Wilcoxon test in the *rpr* suppression study.

genotypes analyzed	n	1	2	3	4	5	6
control (N=217) <i>UAS-rpr/X;vg-GAL4/+</i>	1						
1 copy <i>bcl-2</i> (N=210) <i>UAS-rpr/X;vg-GAL4/+;UAS-bcl-2/+</i>	2	Ws _{1,2} = -4.1 $\alpha_{1,2}$ = 4.9×10^{-5}					
2 copies <i>bcl-2</i> (N=176) <i>UAS-rpr/UAS-bcl-2;vg-GAL4/+;UAS-bcl-2/+</i>	3	Ws _{1,3} = -5.3 $\alpha_{1,3}$ = 1.5×10^{-7}	Ws _{2,3} = -1.0 $\alpha_{2,3}$ = 0.34*				
3 copies <i>bcl-2</i> (N=104) <i>UAS-rpr/UAS-bcl-2;vg-GAL4/UAS-bcl-2;UAS-bcl-2/+</i>	4	Ws _{1,4} = -9.6 $\alpha_{1,4}$ < 1×10^{-13}	Ws _{2,4} = -7.0 $\alpha_{2,4}$ = 1.7×10^{-11}	Ws _{3,4} = -6.8 $\alpha_{3,4}$ = 4.6×10^{-11}			
1 copy <i>p35</i> (N=247) <i>UAS-rpr/X;vg-GAL4/UAS-p35</i>	5	Ws _{1,5} = -5.4 $\alpha_{1,5}$ = 2.4×10^{-12}	Ws _{2,5} = -3.0 $\alpha_{2,5}$ = 3.0×10^{-3} *	Ws _{3,5} = -2.2 $\alpha_{3,5}$ = 0.03*	Ws _{4,5} = 5.5 $\alpha_{4,5}$ = 6.3×10^{-8}		
1 copy <i>bcl-2</i> + 1 copy <i>p35</i> (N=207) <i>UAS-rpr/X;vg-GAL4/UAS-p35;UAS-bcl-2/+</i>	6	Ws _{1,6} = -5.3 $\alpha_{1,6}$ = 1.9×10^{-7}	Ws _{2,6} = -1.1 $\alpha_{2,6}$ = 0.28*	Ws _{3,6} = -0.2 $\alpha_{3,6}$ = 0.82*	Ws _{4,6} = 6.5 $\alpha_{4,6}$ = 2.6×10^{-10}	Ws _{5,6} = 1.9 $\alpha_{5,6}$ = 0.06*	
2 copies <i>bcl-2</i> + 1 copy <i>p35</i> (N=226) <i>UAS-rpr/UAS-bcl-2;vg-GAL4/UAS-p35;UAS-bcl-2/+</i>	7	Ws _{1,7} = -7.7 $\alpha_{1,6}$ = 1.6×10^{-13}	Ws _{2,7} = -3.5 $\alpha_{2,7}$ = 4.3×10^{-4}	Ws _{3,7} = -2.7 $\alpha_{3,7}$ = 5.3×10^{-3} *	Ws _{4,7} = 4.9 $\alpha_{4,7}$ = 9.9×10^{-7}	Ws _{5,7} = -0.7 $\alpha_{5,7}$ = 0.49*	Ws _{6,7} = -2.5 $\alpha_{6,7}$ = 1.3×10^{-2} *

α values noted with * are superior to the significant limit fixed at 1×10^{-3} . The genotypes of the considered distributions are numbered from 1 to 6 (n, grey cells). N specifies the number of flies analyzed.

Table 2: Quantification of the β -galactosidase activity during embryonic development.

development time laps	genotypes analyzed	β -galactosidase activity (mmol ONPG/min/ μ g prot)	standard deviation	α value
0-3h	control (<i>rpr-11-lacZ/da-GAL4</i>)	0.9	0.8	1*
	1 copy p35 (<i>UAS-p35/+;rpr-11-lacZ/da-GAL4</i>)	0.7	0.8	0.48*
	1 copy bcl-2 (<i>UAS-bcl-2/+;rpr-11-lacZ/da-GAL4</i>)	0.6	0.5	0.31*
3-6h	control	2.8	0.9	1*
	1 copy p35	3.2	1.4	0.46*
	1 copy bcl-2	1.6	0.7	0.01
6-9h	control	17.4	6.4	1*
	1 copy p35	18.1	8.3	0.85*
	1 copy bcl-2	7.5	5.7	3.2×10^{-3}

The β -galactosidase activity has been measured 9 times independently (n=9). α values presented here are given by the comparison of the β -galactosidase activity of each genotype analyzed with the activity of the control genotype of the same development time laps. α values noted with * are superior to the statistical significant limit fixed at 0.05.

Table 3: W_s values and α values of the Wilcoxon test for the female lineages in the *bax* suppression study.

females analyzed	n	1	2	3
control (N=101) <i>vg-GAL4,UAS-bax/+</i>	1			
1 copy p35 (N=111) <i>vg-GAL4,UAS-bax/UAS-p35</i>	2	$W_{S_{1,2}} = -0.8$ $\alpha_{1,2} = 0.43^*$		
1 copy bcl-2 (N=93) <i>vg-GAL4,UAS-bax/UAS-bcl-2</i>	3	$W_{S_{1,3}} = -9.1$ $\alpha_{1,3} < 1 \times 10^{-13}$	$W_{S_{2,3}} = -9.3$ $\alpha_{2,3} < 1 \times 10^{-13}$	
3 copies bcl-2 (N=94) <i>UAS-bcl-2/X;vg-GAL4,UAS-bax/UAS-bcl-2; UAS-bcl-2/+</i>	4	$W_{S_{1,4}} = -11.4$ $\alpha_{1,4} < 1 \times 10^{-13}$	$W_{S_{2,4}} = -11.7$ $\alpha_{2,4} < 1 \times 10^{-13}$	$W_{S_{3,4}} = -3.8$ $\alpha_{3,4} = 1.7 \times 10^{-4}$

α values noted with * are superior to the significant limit fixed at 1×10^{-3} . The genotypes of the considered distributions are numbered from 1 to 4 (n, grey cells). N specifies the number of flies analyzed.

Table 4: W_s values and α values of the Wilcoxon test for the male lineages in the *bax* suppression study.

males analyzed	n	5	6	7
control (N=67) <i>vg-GAL4,UAS-bax/+</i>	5			
1 copy p35 (N=64) <i>vg-GAL4,UAS-bax/UAS-p35</i>	6	$W_{S_{5,6}} = 2.6$ $\alpha_{5,6} = 0.01^*$		
1 copy bcl-2 (N=88) <i>vg-GAL4,UAS-bax/UAS-bcl-2</i>	7	$W_{S_{5,7}} = -4.4$ $\alpha_{5,7} = 1.3 \times 10^{-5}$	$W_{S_{6,7}} = -6.6$ $\alpha_{6,7} = 1.6 \times 10^{-10}$	
2 copies bcl-2 (N=117) <i>vg-GAL4,UAS-bax/UAS-bcl-2; UAS-bcl-2/+</i>	8	$W_{S_{5,8}} = -9.0$ $\alpha_{5,8} < 1 \times 10^{-13}$	$W_{S_{6,8}} = -10.3$ $\alpha_{6,8} < 1 \times 10^{-13}$	$W_{S_{7,8}} = -6.0$ $\alpha_{7,8} = 4.9 \times 10^{-9}$

α values noted with * are superior to the significant limit fixed at 1×10^{-3} . The genotypes of the considered distributions are numbered from 5 to 8 (n, grey cells). N specifies the number of flies analyzed.

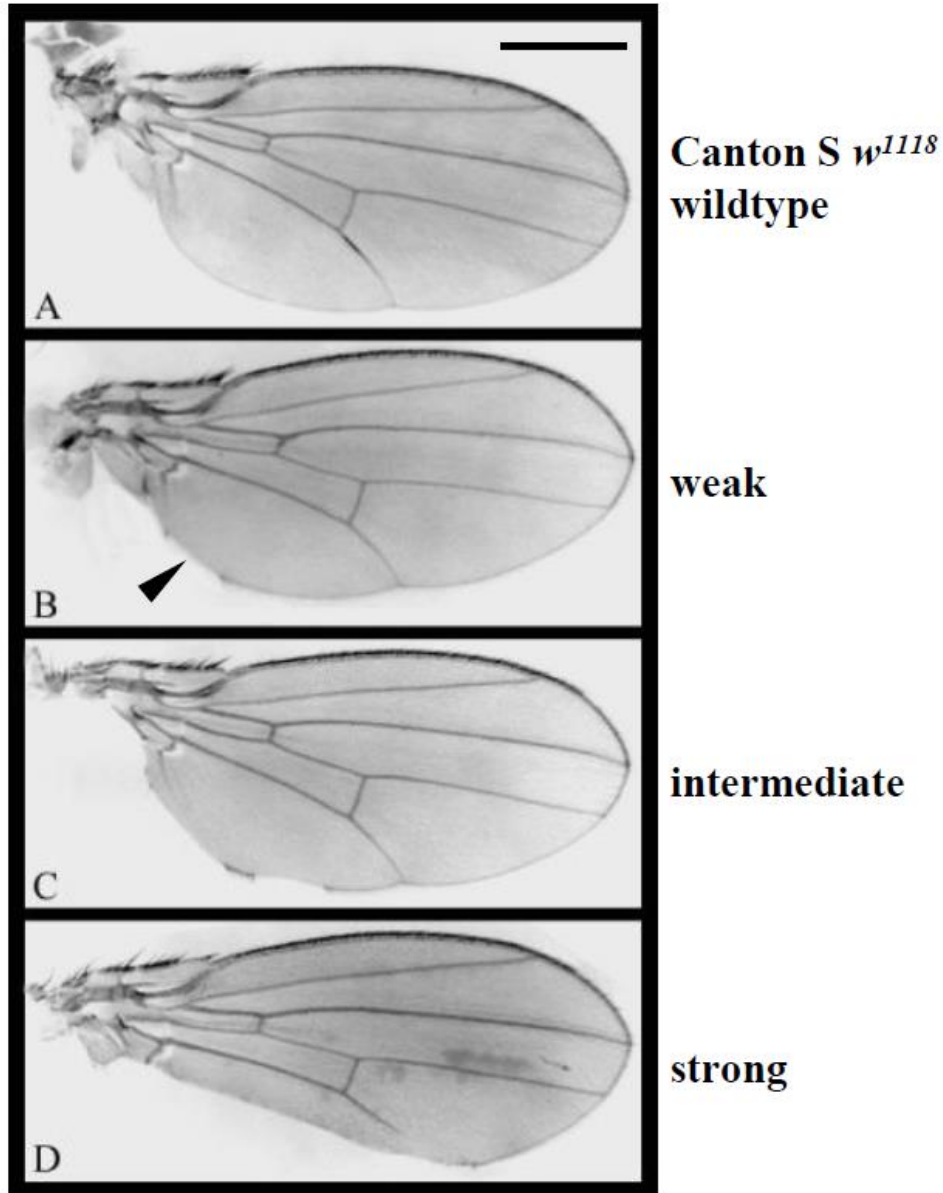


Figure 1: *rpr* induces variable phenotypes in the wing. At 25°C, the phenotypes induced by *UAS-rpr* driven by *vg-GAL4* are variable. We classified flies into four categories based on the strength of their wing phenotype: wildtype (A), weak (B), intermediate (C) and strong (D) phenotypes. In our experiment, the three mutant categories are defined as follows: (A) wildtype wings are similar to these of the Canton S w^{1118} reference strain. Note that the wing in (A) is from the Canton S w^{1118} strain. (B) Wings with weak phenotypes miss only bristles on the proximal posterior margin (arrow head). (C) Wings with intermediate phenotype bear small notches, generally localized on the proximal posterior part of the wing margin. (D) The notches on wings with strong phenotypes are larger extending from the posterior proximal part to the distal part of the wing. (A) Scale bar, 500 μ m.

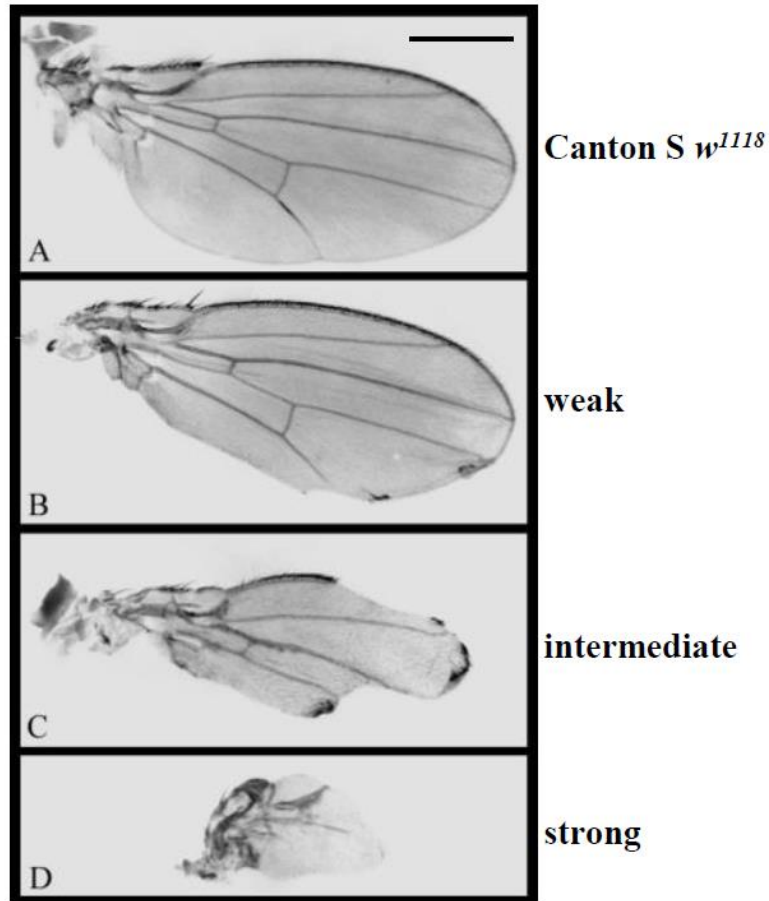


Figure 2: *bax* induces variable phenotypes in the wing. At 18°C, the phenotypes induced by *UAS-bax* driven by *vg-GAL4* are variable. Considering the notches appearing on altered wings, we classified flies into three categories (B,C and D) according to the strength of their wing phenotypes. (A) wildtype Canton S w^{1118} fly wing. (B) The size of a wing with a weak phenotype is almost conserved when compared to wildtype, and the notches are scattered along the margin. (C) The size of a wing with an intermediate phenotype is reduced, and an important part of the margin has disappeared. (D) The strong phenotype is comparable to the *vestigial* phenotype. The wing is partially absent or completely absent, sometimes the flies show thorax abnormalities. Scale bar, 500 μm .

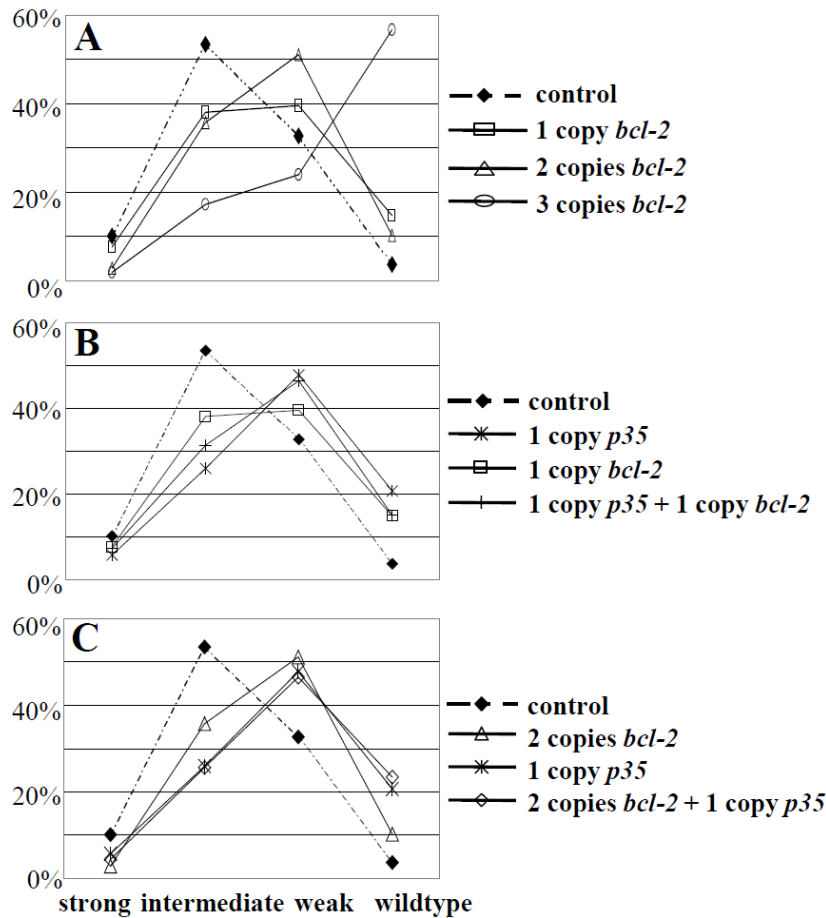


Figure 3: Analyses of the distributions of the phenotypes induced by *rpr*. The percentages of flies listed in each phenotypic category (strong, intermediate, weak and wildtype) are reported in (A), (B) and (C). All flies considered express one copy of *rpr* in the wing as in control ($UAS-rpr/X;vg-GAL4/+$), and one copy of *bcl-2* ($UAS-rpr/X;vg-GAL4/+;UAS-bcl-2/+$), two copies of *bcl-2* ($UAS-rpr/UAS-bcl-2;vg-GAL4/+;UAS-bcl-2/+$) or three copies of *bcl-2* ($UAS-rpr/UAS-bcl-2;vg-GAL4/UAS-bcl-2;UAS-bcl-2/+$) in (A); one copy of *p35* ($UAS-rpr/X;vg-GAL4/UAS-p35$), one copy of *bcl-2* or one copy of *bcl-2* plus one copy of *p35* ($UAS-rpr/X;vg-GAL4/UAS-p35;UAS-bcl-2/+$) in (B); two copies of *bcl-2*, one copy of *p35* or two copies of *bcl-2* plus one copy of *p35* ($UAS-rpr/UAS-bcl-2;vg-GAL4/UAS-p35;UAS-bcl-2/+$) in (C). The statistical Wilcoxon test was used to compare the phenotype distributions (table 1). (A) *bcl-2* partially suppresses the phenotypes induced by *rpr* in a dose-dependent manner. The strength of the phenotypes induced by *rpr* using the *vg-GAL4* driver decreases as the number of *bcl-2* copies increases. (B) and (C), *p35* suppresses *rpr*-induced phenotypes in the wing, but no additive effect on the suppression of *rpr*-induced phenotypes is observed when *bcl-2* and *p35* are co-expressed.

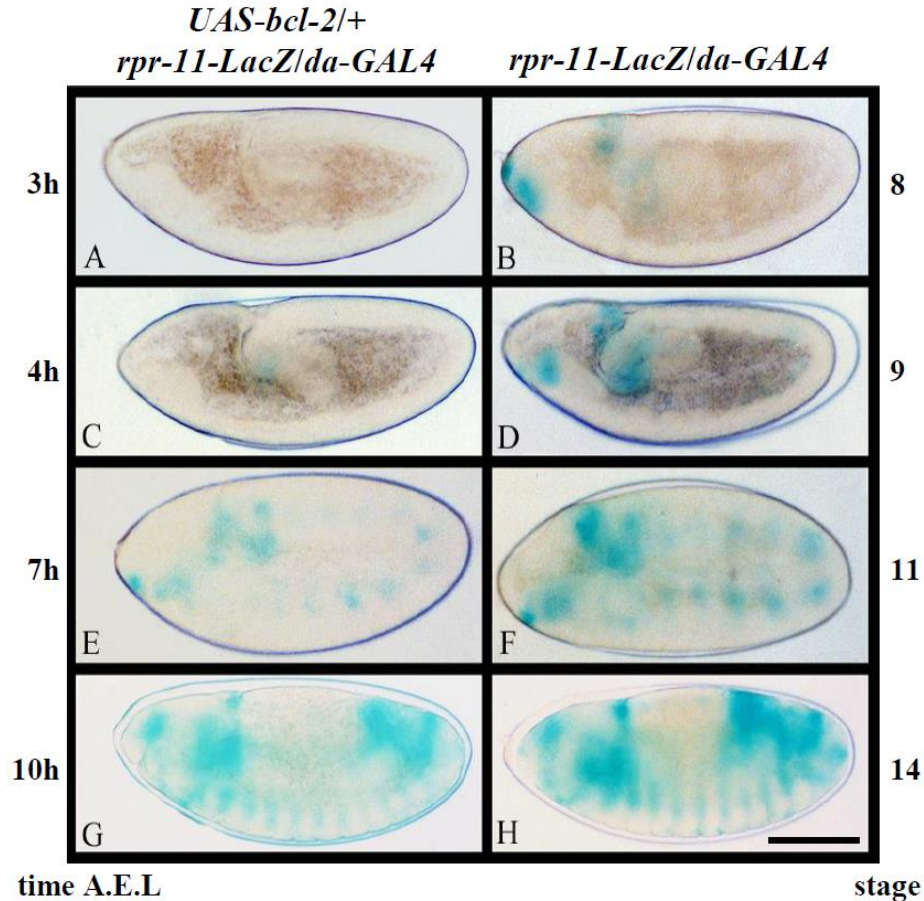


Figure 4: *rpr* repression during embryonic development. We have used the *rpr-11-LacZ* reporter gene (Nordstrom *et al.*, 1996) to study *rpr* expression during embryonic development in embryos expressing *bcl-2*. (A), (C), (E) and (G), embryos expressing the *UAS-bcl-2* transgene under *da-GAL4* control (ubiquitous expression). The approximate times of development and the corresponding stages of development are mentioned on the left and on the right of the figure respectively. The β -galactosidase activity in these embryos is compared to that in control embryos at similar stages (B), (D), (F) and (H). The appearance of β -galactosidase activity is delayed in *bcl-2* embryos until stage 9. At stage 11 and 14, the pattern of *rpr-11-LacZ* is comparable in *bcl-2* embryos (E,G) and in control embryos (F,H), but the β -galactosidase activity is weaker in embryos expressing *bcl-2*. All views are sagittal with anterior to the left and dorsal towards the top. Scale bar, 100 μ m.

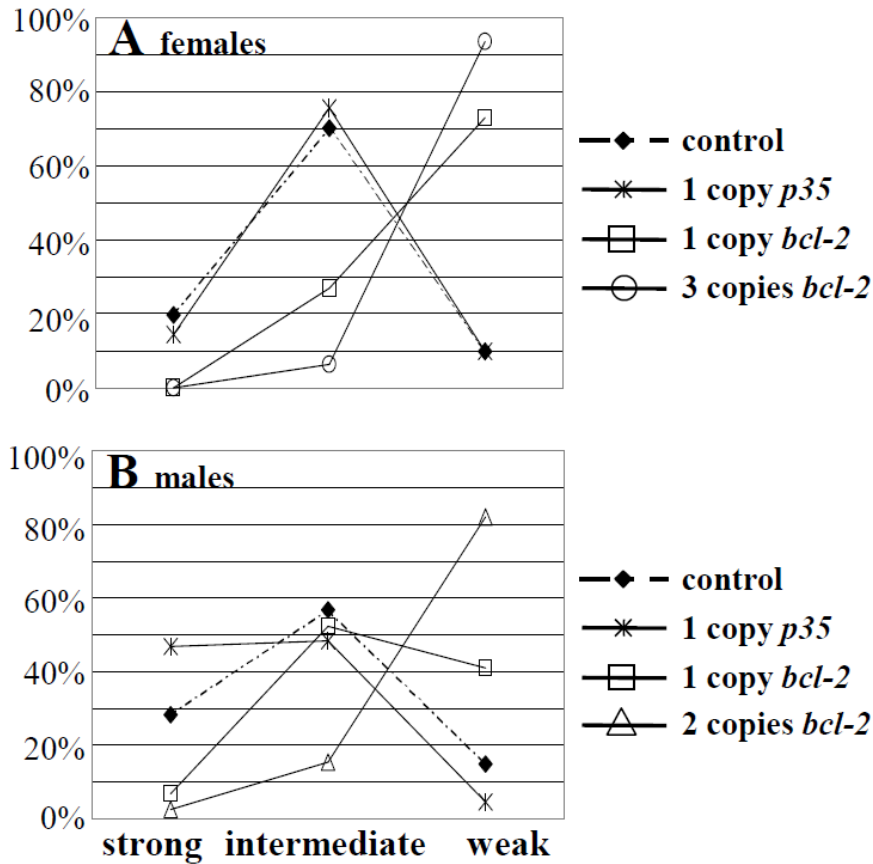


Figure 5: Analyses of the distributions of the phenotypes induced by *bax*. The percentages of flies listed in each phenotypic category (strong, intermediate and weak) are reported in figure 5A and 5B. All flies considered express one copy of *bax* in the wing as in control (*vg-GAL4,UAS-bax/+*) and one copy of *bcl-2* (*vg-GAL4,UAS-bax/UAS-bcl-2*), two copies of *bcl-2* in males (*Y/+;vg-GAL4,UAS-bax/UAS-bcl-2;UAS-bcl-2/+*), three copies of *bcl-2* in females (*UAS-bcl-2/X;vg-GAL4,UAS-bax/UAS-bcl-2;UAS-bcl-2/+*) or one copy of *p35* (*vg-GAL4,UAS-bax/UAS-p35*). The phenotype distributions for the different lineages are compared to each other with the statistical Wilcoxon test (table 3 and 4). (A) In females, *bcl-2* partially suppresses the phenotypes induced by *bax* in a dose-dependent manner while *p35* has no effect. (B) Similarly, in males, *bcl-2* suppresses the phenotypes induced by *bax* in a dose-dependent manner while *p35* has no effect.

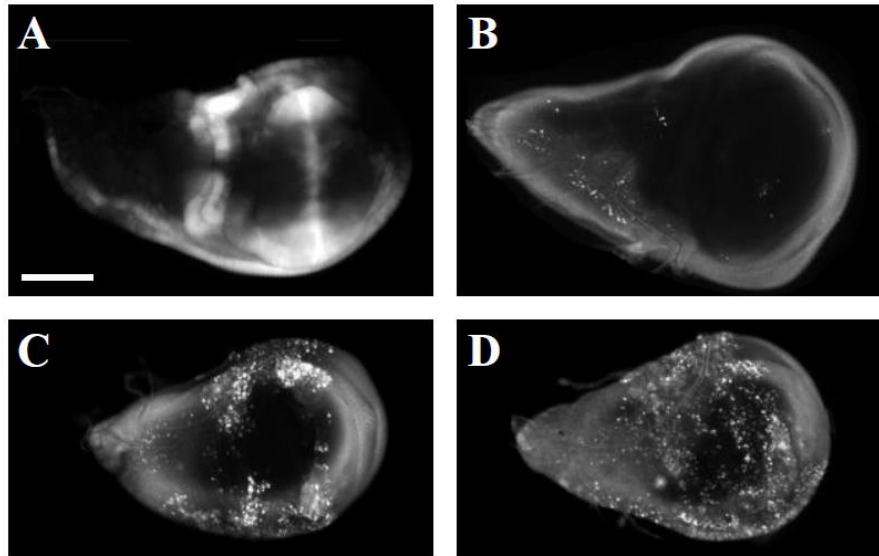


Figure 6: Apoptosis induced by *bax* and *rpr* in wing discs. (A) *vg-GAL4* drives the expression of GFP in an extended zone of (*vg-GAL4/UAS-gfp*) wing disc that corresponds essentially to the future hinge and the future margin of the wing. (B), (C), (D), AO staining of wing discs of third instar larvae. (B), low apoptosis is observed in (*w¹¹¹⁸*) wildtype discs, and most of this apoptosis is localized in the notum. (C), Massive apoptosis is induced in the area of *vg-GAL4* expression in (*UAS-rpr/+;vg-GAL4/+*) wing discs, and (D) in (*UAS-bax,vg-GAL4/+*) wing discs. However, cells in the wing pouch are differently affected by *bax* and *rpr*. All discs are shown with anterior to the top. Scale bar, 100 μ m.

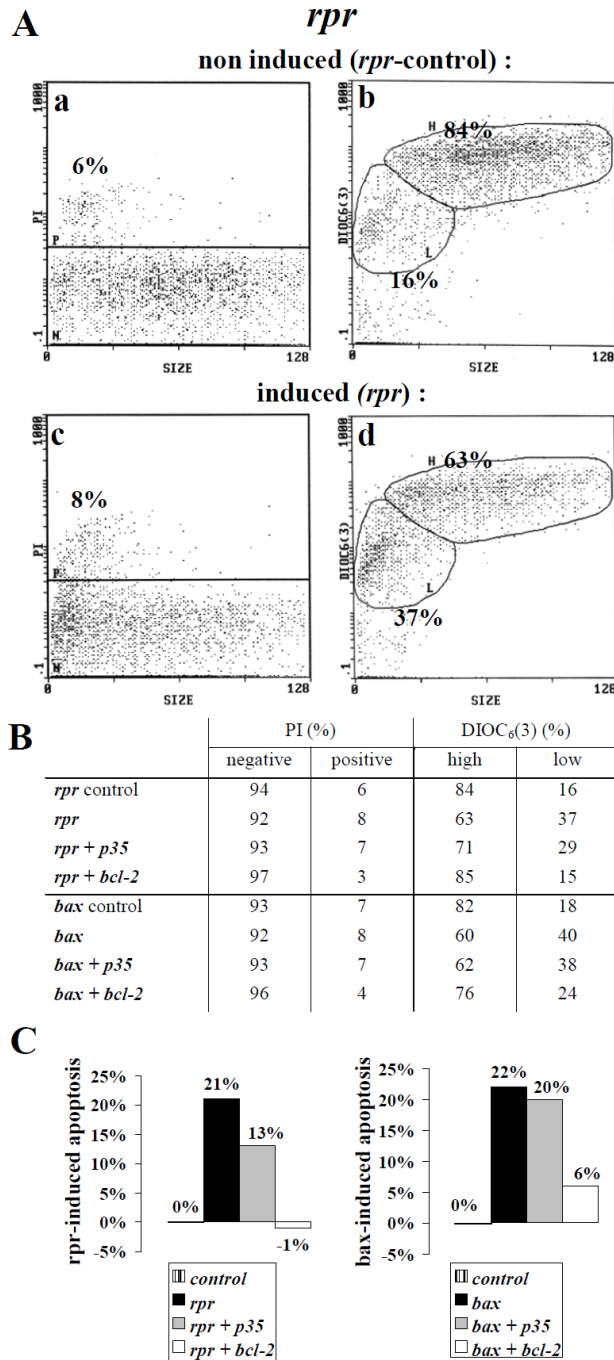


Figure 7: *p35* and *bcl-2* affect mitochondrial changes induced by *bax* or *rpr* expression in wing discs. (A) Multiparametric analysis by flow cytometry of cells extracted from third instar larvae discs. Each dot represents one cell. The data shown are relative to cells extracted from *rpr* control (*UAS-rpr/X*) larvae (a, b) or from (*UAS-rpr/X;vg-GAL4/+*) larvae (c, d). For each sample analyzed, size and membrane integrity, as measured by PI fluorescence (reported in cytograms PI versus size) as well as the mitochondrial membrane potential, as measured by DiOC₆(3) fluorescence (reported in cytogram DiOC₆(3) versus size) were recorded. PI cytograms are separated into two windows, P (upper window) and N which designate PI-positive and PI-negative fluorescent cells respectively. For analysis of DiOC₆(3) fluorescence, only PI-negative cells are considered in multiparametric cytograms, and cells

can be separated into two populations: one with both high fluorescence and large cell size (noted H) and the other with lower fluorescence and reduced cell size (noted L). The percentage of cells in each population is specified. Note that while *rpr* expression induces a loss of mitochondrial membrane potential and a reduction of cell size, PI fluorescence is not affected.

(B) The same analyses have been performed with (*UAS-rpr/X;vg-GAL4/+;UAS-p35/+*) and (*UAS-rpr/UAS-bcl-2;vg-GAL4/+;UAS-bcl-2/+*), *bax* control (*UAS-bax/+*), (*UAS-bax/vg-GAL4*), (*UAS-bax/vg-GAL4;UAS-p35/+*) and (*UAS-bcl-2/X;UAS-bax/vg-GAL4;UAS-bcl-2/+*) larvae. The percentage of cells in populations described in (A) are presented in the table (B) for the different cell samples.

(C) The histograms present the percentage of cells showing a mitochondrial membrane potential decay in window L (low DiOC₆(3) fluorescence) after percentage of the control has been deducted. In these experiments, *bcl-2* can clearly block loss of mitochondrial membrane potential induced by both *rpr* and *bax* whereas *p35* only affects changes in mitochondrial potential triggered by *rpr*. The results obtained have been successfully reproduced.

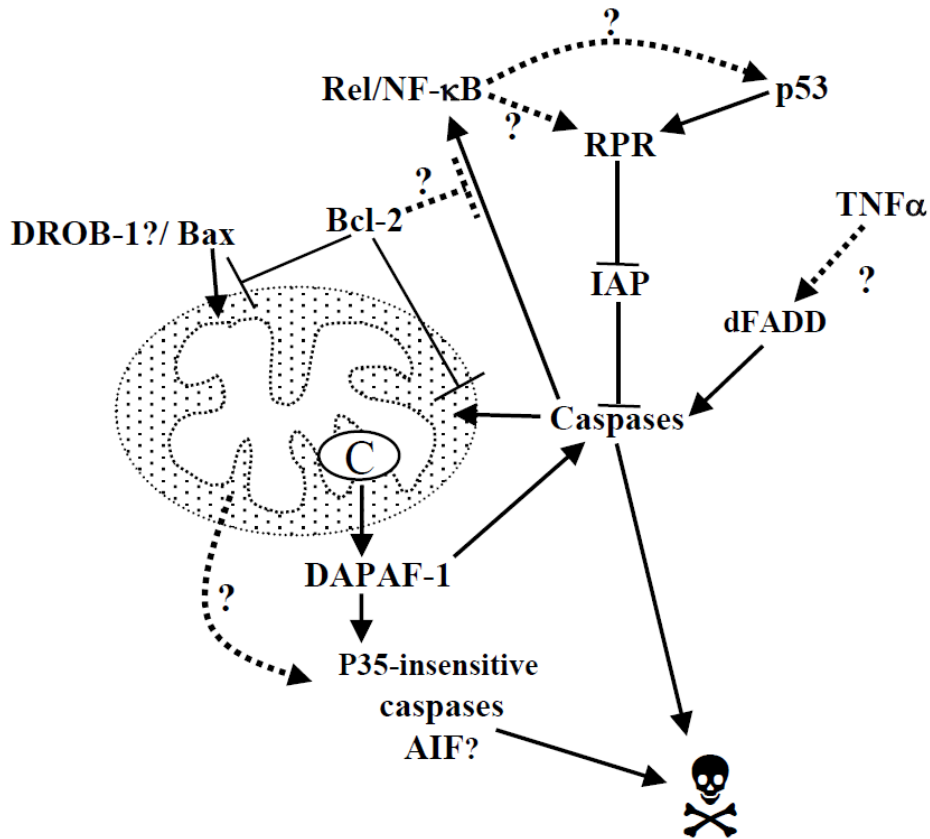


Figure 8: Hypothetical model of apoptosis control in *Drosophila*. This model takes into account the following points : 1) mitochondria are a target of Bax and RPR in *Drosophila*, 2) unlike *rpr*, *bax* induces apoptosis through a *p35*-insensitive pathway 3) Bcl-2 probably acts by counteracting mitochondrial defects triggered by *bax* and *rpr*, 4) a pathway homologous to the TNF α death pathway may exist in the fly (Georgel *et al.*, 2001; Hu & Yang, 2000) and 5) Bcl-2 down-regulates *rpr* expression. This last effect of Bcl-2 might be mediated through the indirect inhibition of Rel/NF- κ B.